On-line Tests of Frame Structures

by

Kenji Kabayama[1)], Manabu Toyoshima[2)], Fumitoshi Kumazawa[3)],
Yoshiaki Nakano[4)] and Tsuneo Okada[5)]

INTRODUCTION

An on-line test is the hybrid method consisting of a numerical simulation of the earthquake response of an analytical model and a loading test of a specimen. The concept of the on-line test was proposed by Dr. Hakuno, M. et al. in 1969[1], and the methodology and its application to structural experiments were developed by Dr. Okada, T. et al. at the Institute of Industrial Science, University of Tokyo in 1973[2]. The on-line test has advantages in dynamic tests of relatively large scale structures over the shaking table test, and it, therefore, has been applied to various seismic experiments of structures.

Although the viscous damping used in the numerical simulation may affect the earthquake response of a specimen, the effect of the viscous damping has often been neglected in on-line tests to simplify the analytical model. It is, therefore, important to investigate the effect to simulate the dynamic response of the specimen in the on-line test precisely.

This paper descries the results of on-line tests of three frame structures which consist of four identical R/C columns. The main objective of this study is to compare the results obtained from the on-line tests and from the shaking table test which was precedingly carried out using the same specimen[3]. In the on-line tests, the damping factor used in the numerical integration was varied to investigate its effect on the seismic behavior of the specimen.

OUTLINE OF ON-LINE TESTS

The testing system consisted of a personal computer to calculate the earthquake response and two actuators, transducers etc. to control loadings as shown in Figure 1.

Three identical test structures consisting of four identical R/C columns, additional R/C weights, a steel table and a steel base as shown in Figure 2 were tested. Details of the R/C column and the mechanical properties of materials are shown in Figure 3 and Table 1, respectively. Each specimen was designed to fail in a ductile manner. The ratio of tensile reinforcement was 2.36%, the ratio of shear reinforcement was 1.54% and the shear-span-to-depth ratio was 3.27. The axial stress in each column was 41.4 kgf/cm^2 which might

---

1) Graduate Student ; Univ. of Tokyo
2) Research Engineer ; Technological Research Center, Tokyu Construction
3) Research Associate ; Institute of Industrial Science, Univ. of Tokyo
4) Associate Professor ; ditto
5) Professor ; ditto

correspond to that of columns in the first story of medium-rise existing R/C buildings in Japan. Each specimen was the same as that used in the shaking table test which was precedingly carried out at the National Research Institute for Earth Science and Disaster Preventions (referred to as NIED hereafter).

The specimen was loaded with two actuators and the deformations of two parallel frames were controlled not to be distorted. The deformation at the tip of the column was monitored and controlled with two kinds of transducers with different stroke capacity and measuring precision. Because the maximum deformation measured during the shaking table test was about 20cm, the transducers with shorter stroke capacity (±5cm) but higher precision were used up to 3cm and then those with longer stroke capacity (± 25cm) were used in the following large deformation range.

The analytical model for a numerical simulation is shown in Figure 4. The Operator Splitting (referred to as OS hereafter) method which was proposed by Dr. Nakashima, M. et al. as a new effective numerical integration method for on-line tests in 1990[4] was used. The equation of motion in the on-line test using the OS method is written as;

$$m\ddot{x}_{i+1} + c\dot{x}_{i+1} + f^{*}_{i+1} + k(x_{i+1} - x^{*}_{i+1}) = -m\ddot{x}_{0i+1} \quad \text{......(1)}$$

where

$$c = 2\omega_0 h \quad \text{......(2)}$$

where m : mass of system, c : coefficient of viscous damping, k : elastic stiffness, $\ddot{x}_{0i+1}$: ground acceleration, $\ddot{x}_{i+1}$: acceleration, $\dot{x}_{i+1}$: velocity, x^{*}_{i+1} : *predictor displacement*, x_{i+1} : *corrector displacement*, f^{*}_{i+1} : restoring force at *the predictor displacement* x^{*}_{i+1}, ω_0 : natural circular frequency, h : damping factor

The predictor displacement x^{*}_{i+1}, *the corrector displacement* x_{i+1} and the velocity $\dot{x}_{i+1}$ are written as follows;

$$x^{*}_{i+1} = x_i + \Delta t\dot{x}_i + \frac{1}{4}\Delta t^2\ddot{x}_i \quad \text{......(3)}$$

$$x_{i+1} = x^{*}_{i+1} + \frac{1}{4}\Delta t^2\ddot{x}_{i+1} \quad \text{......(4)}$$

$$\dot{x}_{i+1} = \dot{x}_i + \frac{1}{2}\Delta t(\ddot{x}_i + \ddot{x}_{i+1}) \quad \text{......(5)}$$

where Δt : time interval

The flow of the on-line test is shown below.

① The displacement x_i, the velocity $\dot{x}_i$ and the acceleration $\ddot{x}_i$ at the current step i are given.
② Compute *the predictor displacement* x^{*}_{i+1} at the next step $i+1$ from Eq. (3).
③ Deform the specimen up to x^{*}_{i+1}.
④ Measure the restoring force f^{*}_{i+1} at x^{*}_{i+1}.
⑤ Compute *the corrector displacement* x_{i+1} of the next step $i+1$ from Eqs. (1), (4) and (5).
⑥ Compute the acceleration $\ddot{x}_{i+1}$ and the velocity $\dot{x}_{i+1}$ from Eqs. (4) and (5), respectively.
⑦ $i = i + 1$
⑧ Return ②.

As shown in Table 2, the damping factor in the Eq. (2) was varied in the experiment, assuming it was proportional to the elastic stiffness calculated from the sectional properties of the R/C column, because it was difficult to estimate the tangent stiffness of the specimen at each loading step accurately.

The accelerogram recorded during the preceding shaking table test was used in this study to facilitate the comparison of both test results. During the shaking table test, the E–W component of 1968 Tokachi–oki Earthquake was used. Figure 5 shows the input accelerogram used in this study.

RESULTS OF ON–LINE TESTS

Crack patterns at the column base and deflection angles around the response time of 4.5 sec. are shown in Figure 6. The deflection angle was 1/120 rad. and many flexural and shear cracks were observed in RC–OL1 (damping factor : h = 0 %), while the deflection angle was 1/300 rad. and only a few flexural cracks were observed in RC–OL3 (h = 3 %).

Hysteresis loops of each specimen are shown in Figure 7. The maximum strength was about 14.4 tonf in each specimen. Hysteresis curves in the large deformation stage, however, differed significantly depending on the numerical assumption, i. e., RC–OL1 (h = 0 %) collapsed in the positive deformation region, RC–OL2 (h = 1 %) in the negative, and RC–OL3 (h = 3 %) did not collapse. It reveals that the response of each specimen is highly depending on the damping factor assumed in the numerical integration.

COMPARISON WITH THE SHAKING TABLE TEST

As previously stated, the shaking table test with the same specimen was carried out at NIED. The response displacement waveforms recorded during the shaking table test (referred to as STT hereafter), RC–OL1 (h = 0 %) and RC–OL3 (h = 3 %) are compared in Figure 8. This figure shows that RC–OL3 (h = 3 %) simulates well the STT result within the first 6 sec. but RC–01 (h = 0 %) then gradually compares well with the STT result in the following time. It indicates that the viscous damping has a significant effect on the response of the specimen and that it should be varied depending on the damage level of specimen, rather than constant as assumed in the test herein, to simulate the dynamic response precisely.

CONCLUDING REMARKS

On–line tests of frame structures consisted of four R/C columns were carried out using the OS method as a numerical integration method. The results of these tests were compared with those of the preceding shaking table test. The major findings are summarized as follows;

① The response of the specimen is highly depending on the damping factor assumed in the numerical integration.

② The viscous damping should be varied depending on the damage level of the specimen to simulate the dynamic response precisely.

REFERENCES

[1] Hakuno, M., Shidawara, M. and Hara, T. : Dynamic destructive test of a cantilever beam, controlled by an analog–computer, Transactions, Japan Society of Civil Engineerings, No.171, pp.1–9, Nov. 1969.

[2] Okada, T. and Seki, M. : Nonlinear earthquake response of reinforced concrete building frames by computer–actuator on–line system (Part 1 Objective and methodology), Transactions, Architectural Institute of Japan, Tokyo, Japan, No.275, pp.25–31, Jan. 1979.

[3] Kogoma, I., Hayashida, T. and Minowa, C. : Experimental studies on the collapse of RC columns during strong earthquake motion, Proceedings of 10th WCEE, Vol.5, pp.3013–3017, Jul. 1992.

[4] Nakashima, M., Ishida, M. and Ando, K. : Integration techniques for substructure pseudo dynamic test (Pseudo dynamic test substructuring techniques), Journal of Structural and Construction Engineering, Transactions, Architectural Institute of Japan, Tokyo, Japan, No.417, pp.107–117, Nov. 1990.

Table 1 Mechanical properties of materials

Concrete

Test Name	Compressive Stress (kgf/cm^2)	Young's Modulus (kgf/cm^2)
RC-OL1, RC-OL2	447	2.67×10^5
RC-OL3	418	2.65×10^5

Reinforcement

	Yield Stress (kgf/cm^2)	Tensile Stress (kgf/cm^2)	Young's Modulus (kgf/cm^2)
D6	3750	5160	1.74×10^6
D16	3780	5550	1.83×10^6

Table 2 Test name and damping factor

Test Name	Damping Factor (h)
RC-OL1	0%
RC-OL2	1%
RC-OL3	3%

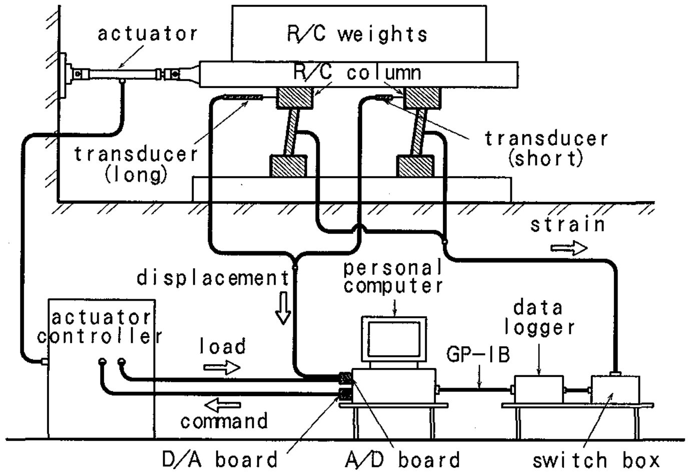

Figure 1 Outline of testing system

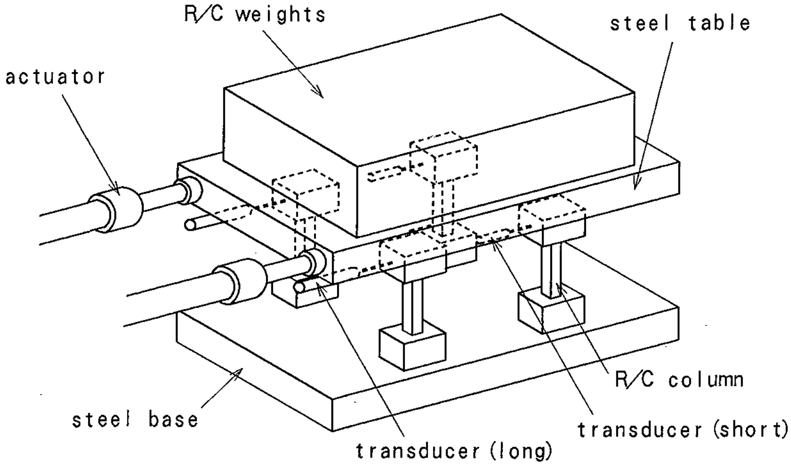

Figure 2 Frame structure

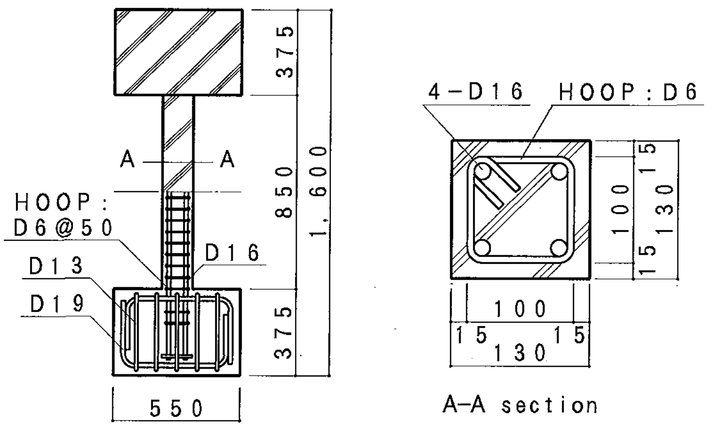

Figure 3 Details of R/C column

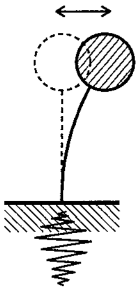

weight: M = 27.99 tf　damping factor: h... varied

stiffness: k = 39.06 tf/cm　gravity acceleration: g = 980 cm/sec^2

mass: $m = \frac{M}{g} = 0.0285$ tfsec^2/cm

natural circular frequency: $\omega_0 = \sqrt{\frac{k}{m}} = 37.02$ rad./sec

coefficient of viscous damping: $c = 2\omega_0 h$

Figure 4 Analytical model

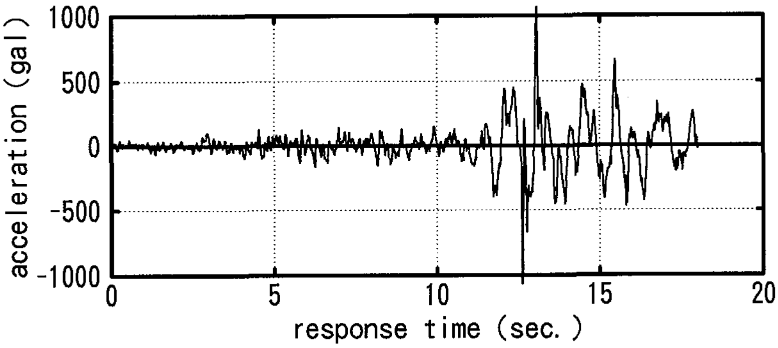

Figure 5 Input accelerogram

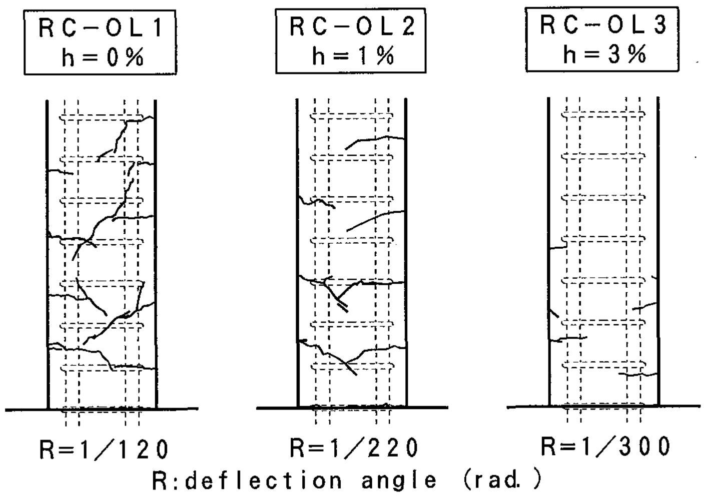

Figure 6 Crack patterns at the column base around the response time of 4.5 sec.

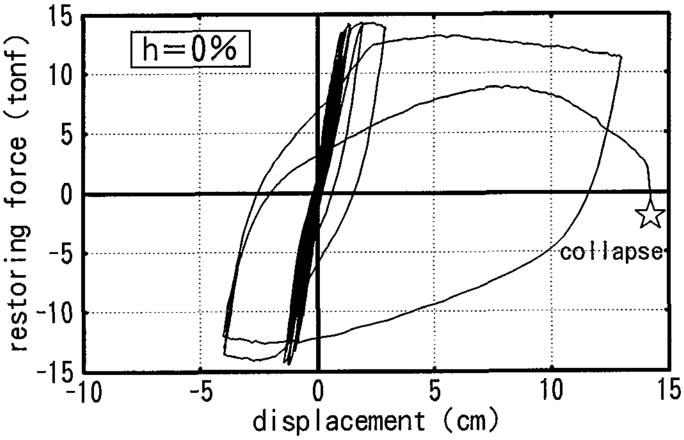

(a) RC-OL1 (h=0%)

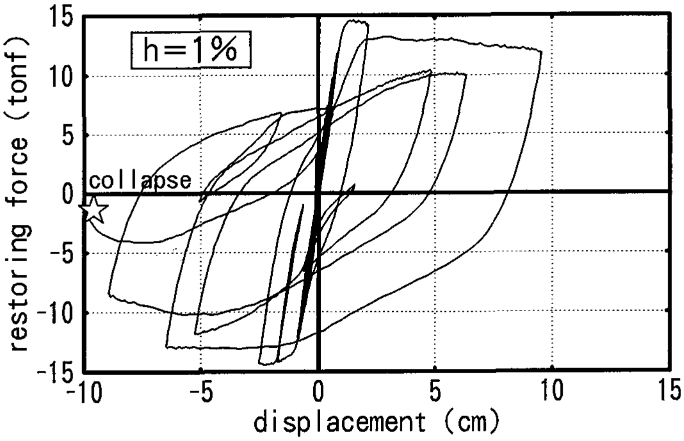

(b) RC-OL2 (h=1%)

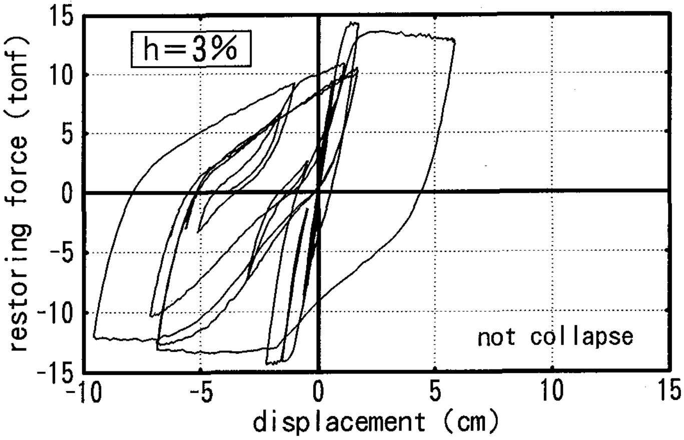

(c) RC-OL3 (h=3%)

Figure 7 Hysteresis loops

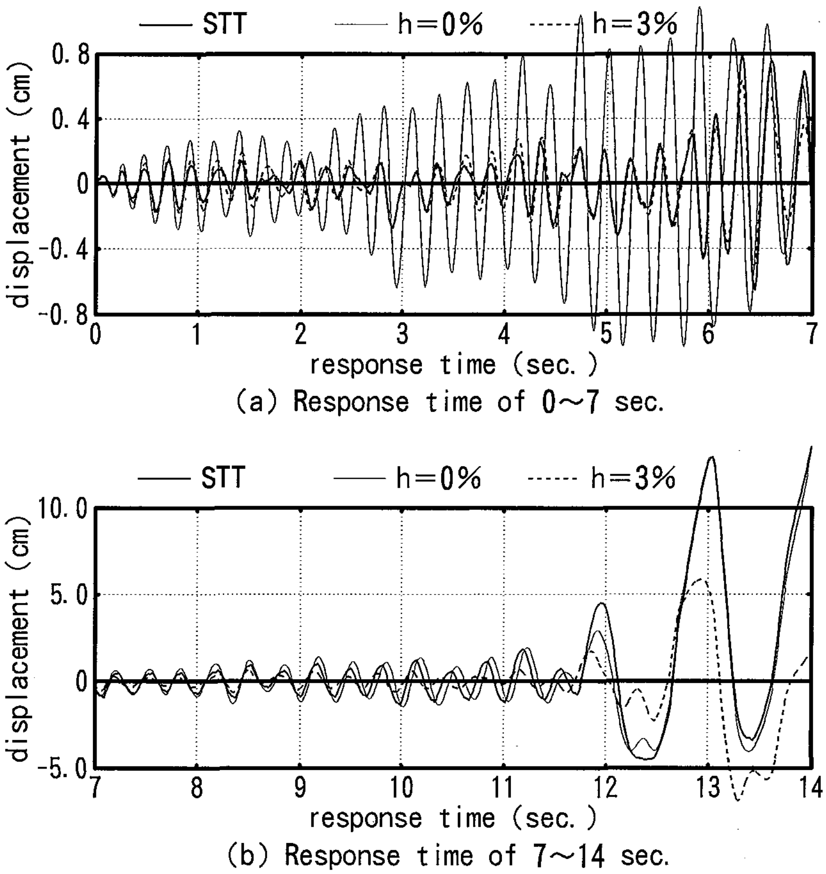

Figure 8 Comparison of response diplacement waveforms